JOURNAL OF PROPULSION AND POWER
Vol. 18, No. 4, July–August 2002

Analysis of a Fusion-Electric Airbreathing Earth to Orbit Launch Vehicle

Robert B. Adams*
International Space Systems, Inc., Huntsville, Alabama 35816
and
D. Brian Landrum†
University of Alabama in Huntsville, Huntsville, Alabama 35899

A novel, advanced airbreathing propulsion system, the simultaneous heating and expansion (SHX) engine, is proposed. The SHX uses coherent beam emitters to couple energy generated by a fusion reactor to the engine flowpath. A quasi-one-dimensional model was developed to calculate axial flow properties in the inlet, combustor, and expansion sections. Models were developed for three different beam emitters: an HF laser, CO_2 laser, and electron beam. Mass relations for the engine components were derived from the literature. SHX simulations produced similar performance to an idealized scramjet, but superior performance in comparison to a baseline fusion rocket. These results indicate the SHX concept could potentially provide the significant performance increase required to meet launch cost goals set by NASA and is worthy of further study.

Nomenclature

A = cross-sectional area, m^2
F = thrust, N
h = enthalpy, J/kg; height of engine inlet, m
I = beam intensity, W
I_{sp} = specific impulse, s
l = length of engine inlet, m
m = mass, kg
P = power, W
p = pressure, Pa
q = heat input per unit mass, J/kg
R = gas constant, J/kg · K
Sa = stream thrust function, m/s
ST = specific thrust, m/s
s = entropy, J/kg · K; path variable, m
T = temperature, K
u = velocity in x direction, m/s
α = absorptive coefficient, 1/m
ρ = density, kg/m^3

Subscripts

c = combustor
e = expander
el = beam emitter
fs = fusion system
i = inlet
th = thrust chamber
0 = conditions at nose of vehicle
10 = conditions at expansion area discharge

Received 1 December 2000; revision received 21 January 2002; accepted for publication 12 February 2002.

*Systems Engineer, 500 Wynn Drive, NW, Suite 306; currently, NASA Marshall Space Flight Center, Huntsville, AL. Member AIAA.

†Associate Professor, Department of Mechanical and Aerospace Engineering, Propulsion Research Center, Tech Hall S234. Senior Member AIAA.

Introduction

SPACE exploration in the 21st century will require more cost-efficient launch systems for placing payloads into Earth orbit. These approaches typically involve increasing engine efficiency and, thus, payload mass. This mass increase could also be used for additional systems to increase redundancy (and thereby increase safety) and to reduce operations requirements. Various rocket and turbine-based airbreathing launch propulsion concepts have been proposed. However, most of these concepts do not provide the significant performance increases required to meet the aggressive cost goals set by NASA.

This paper describes an advanced airbreathing propulsion system called the simultaneous heating and expansion (SHX) engine. The SHX concept uses a coherent-energy beam, such as a laser or electron gun, to deposit energy into the working air. A fusion reactor generates the energy to avoid the complications of fission reactors. The engine flowpath is designed with a changing axial area profile to alleviate thermal choking due to energy deposition. The result is an engine flow that receives large amounts of power from a compact energy source. The flow experiences minimal obstructions and can be expanded while heating to produce a high-energy exhaust. The resultant thrust may be suitable for launch applications either as primary propulsion or for thrust augmentation.

The SHX offers several potential advantages over traditional airbreathing systems. The compact fuel source eliminates the need for large, heavy fuel tanks typical of current systems. Less tankage produces smaller vehicles, thereby realizing an aerodynamic advantage. The SHX may potentially operate over a greater Mach number range than current airbreathing engines. Should this prove true, the SHX could replace several airbreathing cycles in a combined cycle system, thereby simplifying the overall engine.

Analysis of all of the potential advantages would require simulation of the SHX performance for several vehicle concepts through a full trajectory. This feasibility study compares SHX performance to a conventional scramjet at a point in a typical flight trajectory of a combined cycle propelled launch vehicle. To accomplish this, the authors created a computer model that calculates the gasdynamic properties of the SHX propulsion flowpath from the vehicle tip to tail. The simulation also models the mass–power relations for the fusion and beam emitter subsystems. A complementary simulation of an idealized scramjet engine was performed for comparison purposes.

Note that a practical fusion reactor is not in operation today. The SHX concept anticipates the difficulties with maintaining a

fusion reaction will be overcome, and a viable, flight-capable fusion system will eventually be deployed. Until that happens, the research described herein can help address the systems engineering issues of using a fusion source in a highly efficient Earth to orbit vehicle.

SHX Simulation Model

Overview

The SHX model simulates the gasdynamics of the tip to tail engine flowpath. The model also calculates engine performance and weight and power requirements for the fusion power and beam emitter subsystems. Figure 1 shows a theoretical SHX powered vehicle. The engine flowpath can be divided into several regions, each involving different underlying phenomena. Stations are defined with numeric designations for the interfaces between the flowpath components consistent with those defined by Heiser and Pratt.[1] Each of the regions illustrated in Fig. 1 is described in the following sections.

Fusion Reactor

Several reactor concepts are currently being researched, with the potential to achieve practical fusion in the near future. One promising concept is the quiet electric discharge (QED) system,[2] which uses inertial electrostatic confinement to achieve fusion. Figure 2 illustrates an expanded view of the fusion chamber and electrical conversion diagram. Injecting electron beams creates a negative potential well in the center of the fusion chamber. The well is restrained by an externally applied electric field created by concentric grids inside the fusion chamber. The charged particles generated in the fusion reaction push against the electric field. The resultant interaction creates a voltage differential that can be used for power production. Bussard assumed a p–B^{11} reaction for the QED concept, primarily because it is aneutronic.[2] However, this reaction is also very difficult to ignite.[3]

Bussard developed several empirical equations that predict the component weights of a QED fusion engine.[2] To allow power system scaling, each weight is defined as a function of a nondimensional ratio of the fusion reactor power output to a reference power,

$$P_0 = P/2150 \cdot \text{MW} \tag{1}$$

The th mass relation to the design power is defined by

$$m_{\text{th}} = 400P_0 + 100P_0^{1.67} + 40 \text{ kg} \tag{2}$$

This relationship includes mass estimates for the beam optics and the propellant turbopump assembly. The fusion power source mass is modeled by

$$m_{\text{fs}} = 250P_0 + 550P_0^{0.5} + 600 \text{ kg} \tag{3}$$

This mass component includes the reactor, the magnetic field generators, and the structural shell.

Bussard's QED rocket concept used an electron beam to heat the fuel.[2] The current SHX concept uses lasers or an electron gun assembly. It is assumed that the electron gun weight is roughly comparable to the weight of a laser assembly at the same total beam strength. The method for creating and focusing a beam (whether laser or e-beam) is herein referred to as the beam emitter subsystem. Its mass is modeled by

$$m_{\text{el}} = 1800P_0^{1.67} \text{ kg} \tag{4}$$

The total engine assembly mass,

$$m_{\text{total}} = m_{\text{th}} + m_{\text{fs}} + m_{\text{el}} \tag{5}$$

is used as a conservative estimate of the total SHX engine weight for calculating thrust-to-weight parameters.

The fusion system is considered a black box that produces the power necessary to drive the SHX engine. The mass–power relationships presented comprise the extent of fusion power analysis in this study.

Inlet Section

To allow a direct comparison between the SHX and scramjet models, the same two-shock external–internal inlet design was used for both (see Fig. 1). The air throughout the inlet flowpath is assumed to be a calorically perfect gas. In addition, the inlet is assumed to operate at design conditions, that is, the bow shock is always on the cowl lip. To maintain this condition, the optimal inlet length l_i and area A_0 are considered variables to be calculated by the program. The bow shock is reflected by the cowl lip and terminates at the junction of the inlet compression ramp and the

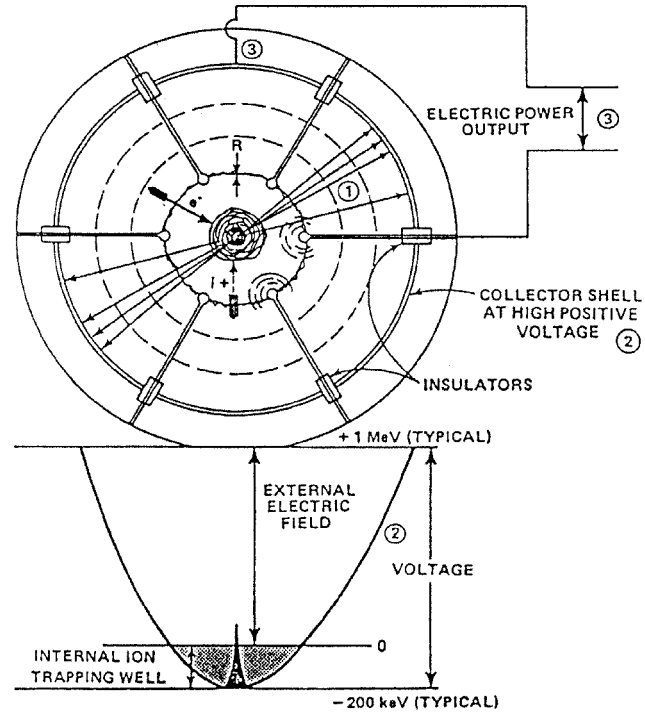

Fig. 2 QED fusion chamber and electrical conversion diagram.[2]

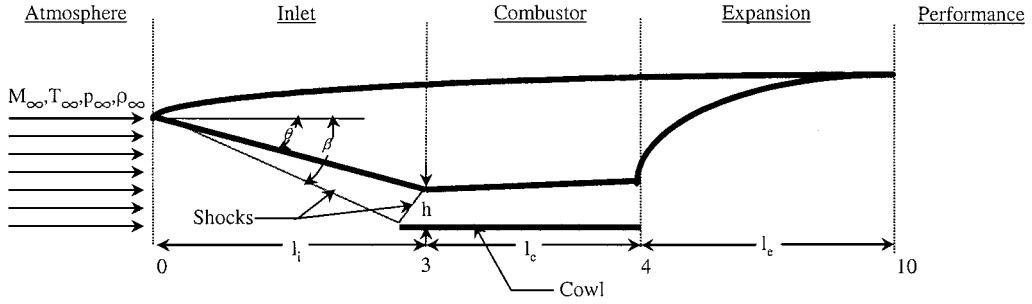

Fig. 1 Schematic of baseline SHX vehicle geometry.

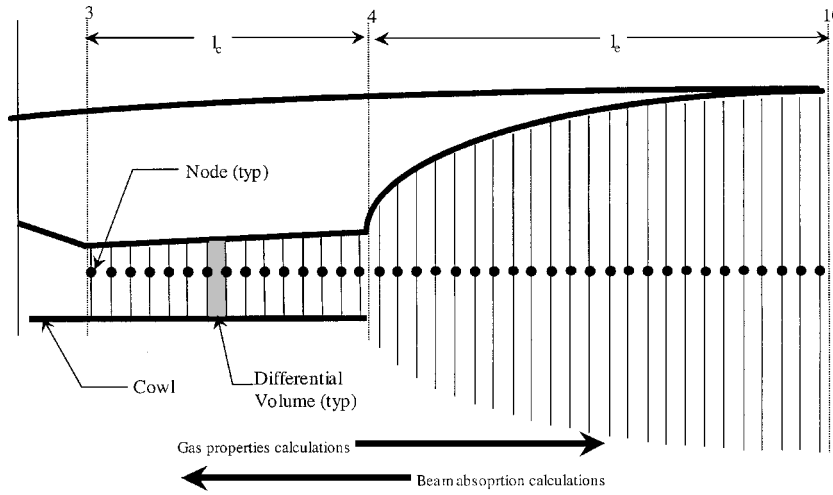

Fig. 3 Schematic of combustor and expansion sections showing differential volumes.

combustor duct. The assumption of design condition operation precludes an off-cowl shock, which would introduce a complex two-dimensional flow. Although not valid for a full trajectory profile, this assumption is sufficient for the point solutions analyzed in this study.

Combustor/Expansion Section

As discussed in Ref. 4, the equations to calculate the fluid properties in the combustor and expansion sections are derived assuming the flow is steady, supersonic, inviscid, and quasi-one-dimensional with heat addition. The combustor and expansion sections are divided into differential volumes as illustrated in Fig. 3. Under the assumption of sufficiently small differential volumes, a linear relationship between pressure and area replaces the pressure integral in the momentum equation. The resultant quasi-one-dimensional governing equations for mass, momentum, and energy in a differential volume of axial length Δx are

$$\rho_x u_x A_x = \rho_{x+\Delta x} u_{x+\Delta x} A_{x+\Delta x} \tag{6}$$

$$\left\{\rho_x u_x^2 A_x + p_x A_x + [(p_{x+\Delta x} + p_x)/2](A_{x+\Delta x} - A_x)\right\} = \left[\rho_{x+\Delta x} u_{x+\Delta x}^2 A_{x+\Delta x} + \cdots + p_{x+\Delta x} A_{x+\Delta x}\right] \tag{7}$$

$$h_x + u_x^2/2 + q = h_{x+\Delta x} + u_{x+\Delta x}^2/2 \tag{8}$$

Figure 4 illustrates the passage of a laser beam through a representative control volume. In an operational system, multiple beams would be projected through the volume at different angles to meet the propulsion system heating requirements. The SHX model assumes that the total beam energy is dispersed uniformly over the engine duct's cross-sectional area at every point in the flow. In this manner we can also assume that the beam path distance Δs, shown in Fig. 4, is approximately equal to the volume length Δx.

The model for beam attenuation and airflow heating is presented in Ref. 4. The resultant heat addition in a volume can be defined as a function of beam attenuation, absorption coefficient, and gas properties as

$$q = \frac{I\alpha\Delta s}{\rho_x u_x A_x} \approx \frac{I_{x+\Delta x} - I_x}{\rho_x u_x A_x} \tag{9}$$

Solutions for both frozen and equilibrium flow are calculated. The actual flow is bracketed between these two solutions.[5] The supersonic flowpath calculations must proceed moving downstream from the fore toward the aft of the vehicle. However, the energy beams are directed axially from the aft toward the front of the

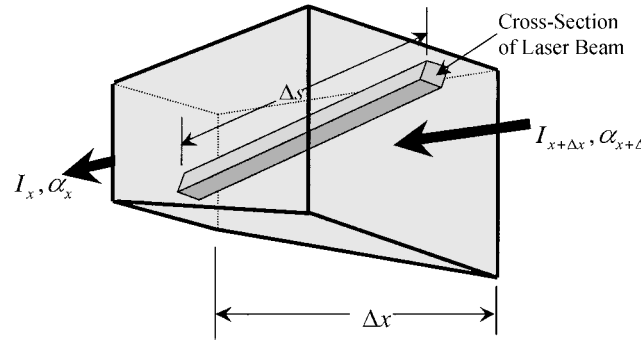

Fig. 4 Differential volume showing beam geometry.

combustor section. An iterative solution, illustrated by opposing arrows in Fig. 3, is, therefore, required because both calculations are coupled through the beam absorption coefficient and attenuation profile. This iterative method is described in greater detail in Ref. 4.

One concern is the reflection of incident beams off of the engine walls. Brown et al.[6] suggest that a laser beam will be refracted away from the wall by the high-density gradients in the hot boundary layer. Therefore, laser heating of the engine walls is neglected in the current analysis.

The flowpath axial area profiles shown in Fig. 5 are defined through user-specified parameters. Currently, there are three area profile options: bilinear, parabolic, and constant slope. The inlet section is the same for all options. The bilinear option assumes that the area varies linearly with axial distance in both the combustor and expansion sections. The slopes for each section are derived from the user-defined area ratios (A_4/A_3 and A_{10}/A_4). The parabolic option assumes the same linear profile for the combustor section as the bilinear case, but the expansion section varies proportionally with $\sqrt{x}$. This option was designed to represent more accurately expansion section contours found in typical airbreathing concepts. The final area option assumes a constant slope across both the combustor and expansion sections. This slope is derived from the product of the combustor and expansion area ratios (A_{10}/A_3).

Performance Parameters

Comparison between the SHX and existing propulsion concepts requires an understanding of several engine performance parameters. Because the mass of fuel injected into the airstream is assumed to be negligible, the mass flow rate remains constant throughout the engine flowpath. The stream function is defined as the

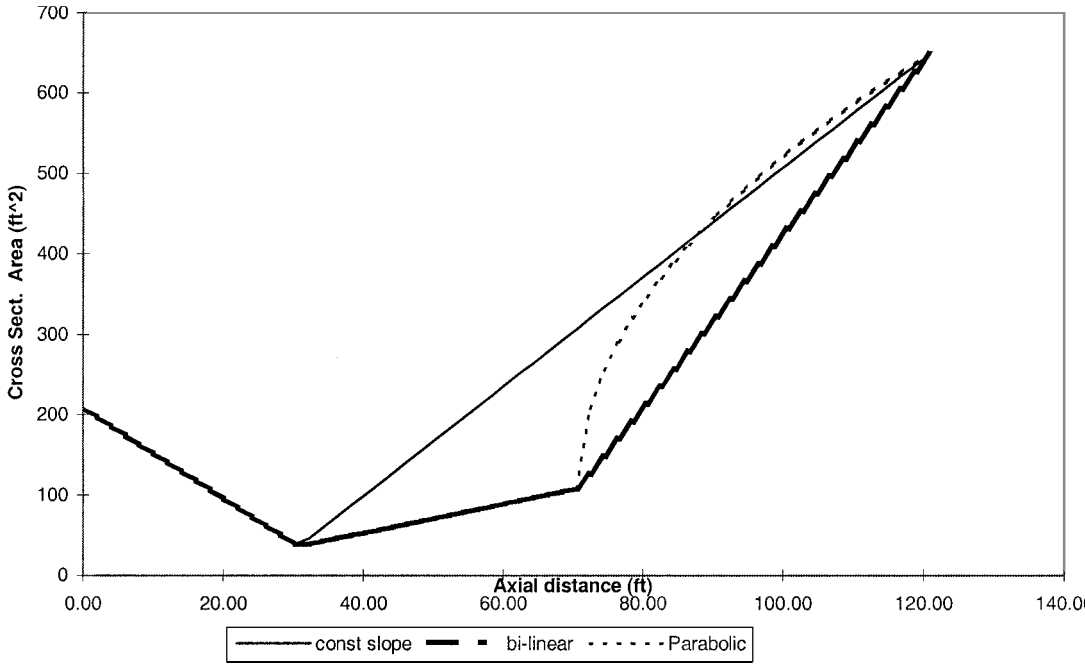

Fig. 5 Axial area profiles for the SHX combustor and expansion sections.

thrust force per unit mass flow rate of air at a specific operation point,[1]

$$Sa = u(1 + RT/u^2) \tag{10}$$

The engine's net thrust is determined by a momentum balance between the incoming and outgoing airstream and can be found using the stream functions at those points. Based on the properties at stations 0 and 10 (see Fig. 1), the net thrust is given by

$$F = [(Sa_{10} - Sa_0) - (R_0T_0/u_0)(A_{10}/A_0 - 1)]\dot{m} \tag{11}$$

Specific thrust is a performance parameter frequently used in lieu of specific impulse for airbreathing vehicles. It is defined as the thrust per mass flow rate of ingested air,

$$ST = F/\dot{m}_{\text{air}} \tag{12}$$

This parameter can be used for engine scaling purposes. The engine inlet is sized to provide an air mass flow for the required thrust. Obviously, the highest possible ST values are desired.

The engine thrust-to-weight (T/W) ratio is another measure of performance. Because the engine and fuel comprise the major portion of the vehicle weight, this parameter also estimates the vehicle acceleration in multiples of Earth's gravity experienced at liftoff.

The specific impulse is the total impulse that the engine can deliver divided by the weight flow of the propellant,[1]

$$I_{\text{sp}} = F/\dot{m}_f g \tag{13}$$

Specific impulse is by far the most popular parameter used for comparing propulsion systems. However, it is difficult to apply this parameter to the SHX because the engine burns fuel at a negligible rate. For example, an 8000-MW fusion reactor operating with a $D + He^3$ reaction would consume only 0.008 kg of fuel over a 6-min flight time. Even accounting for inefficiencies in the reaction and power conversion, it is clear that this mass is insignificant. Estimates of specific impulse based on fusion fuel expended would not give an accurate representation of the effectiveness of the SHX.

Beam Emitters

Coupling of the heating mechanism with the working airflow in the SHX engine is a function of the type of beam, absorption coefficients, and the gas properties. Obviously, high absorption coefficients are desired to facilitate air heating. Three different beam types have been identified as potentially suitable for this engine concept: a hydrogen–fluorine (HF) laser, a carbon dioxide (CO_2) laser, and an electron beam (e-beam). Each of these is described in further detail hereafter.

HF Laser

The HF chemical laser has the potential for very high-power operation. The HF reaction produces vibrationally excited molecules, which release energy through emitting quanta. The majority of the quanta are concentrated in the 2.7–2.8 μm band, which is strongly absorbed by the CO_2 present in the air. Expanding the air then converts this thermal energy into flow kinetic energy.

Miles et al.[7] derived absorption coefficients from the HITRAN model.[8] They assumed the laser energy is concentrated at a wavelength of 2.76 μm. Macheret et al.[9] reported experimental results that indicate high-pressure effects act to increase the absorptivity. They also found that the HITRAN database underpredicted the absorption coefficients. Macheret et al. attributed the underprediction to the HITRAN database not accounting for secondary excitation modes between the atmospheric molecules and the incident beam.

With the data reported in Ref. 6, a relationship between absorption coefficients and the local gasdynamic properties was determined.[4] Charts published by Miles et al.[7] showed pressure and temperature data vs axial position for a wind-tunnel section heated by an HF laser. Total enthalpy values calculated from these properties led directly to determining the energy absorbed between axial stations. Equation (8) was used to calculate the power of the incident beam at each axial station. Absorption coefficients were then found at each axial station using Eq. (9). The chemical equilibrium analysis (CEA) code[10] was used to derive air densities for the temperatures and pressures given in Ref. 6. Figure 6 shows the resultant absorption coefficient data plotted vs density, along with a series of polynomial curve fits used in the HF beam model.

Most HF laser assemblies are designed to operate with an open mass loop. However, in this approach, the mass of reactants required to propel a transatmospheric vehicle would not offer any advantages over a chemical rocket. To close this loop requires a means

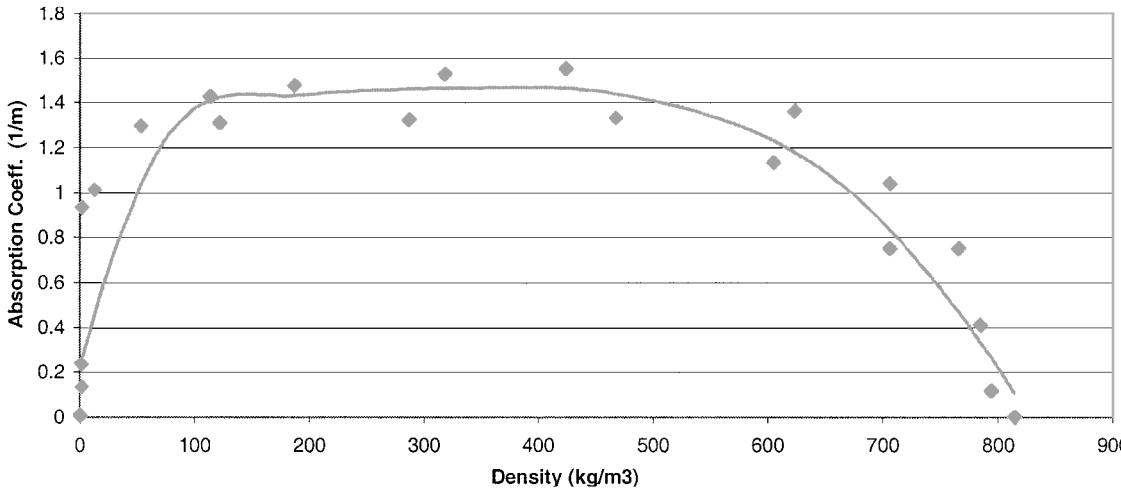

Fig. 6 Calculated absorption coefficients of air vs density for HF laser energy at 2.76 μm; polynomial curve fits are shown by solid lines.

of disassociating the HF downstream of the laser cavity and recycling the constituents. Pumping the HF through the cooling coils surrounding the fusion reactor might provide the disassociation energy. The masses of the cooling coils, pumps, and other equipment are already accounted for in the fusion reactor mass equations. It is assumed that the laser optics system is comparable in mass to the equipment necessary to generate an electron beam. Therefore, the only new mass introduced by the use of an HF laser is that of the hydrogen and fluorine reactants and the helium dilutent.

Gastaud et al.[11] reported H_2, F_2, and He mass flow rates for a specified HF laser beam power. Scaling these values to the power requirements of the baseline SHX vehicle yields a total reactant mass flow rate. Computing the total reactant mass from the mass flow rate requires multiplication by a cycle time. The authors assumed a time to cycle throughout the reactant loops of 0.1 s. This assumption is addressed in Ref. 4.

CO_2 Laser

The second approach considered for coupling energy to the SHX airflow involves the use of a CO_2 laser. This laser is similar to the HF laser in that there is a gaseous medium being stimulated to emit quanta.[12]

Atmospheric air tends to be transparent to the wavelengths generated by CO_2 lasers. CO_2 and H_2O are the only two molecules in the atmosphere that have appreciable absorptive cross sections. Duley[12] reported CO_2 and H_2O absorption coefficients for a wavelength of 10.59 μm. The authors normalized those equations to density to obtain

$$\alpha_{CO_2} = 1.44 \times 10^{-3}(0.835\rho)^{1.5} \exp[-2.747\rho\, \ell n(10)] \text{ 1/cm} \quad (14)$$

$$\alpha_{H_2O} = 4.32 \times 10^{-11} p(641.606\rho + 193p) \text{ 1/cm} \quad (15)$$

Here, density is in units of kilograms per cubic meter, and p represents the partial pressure of water in torr.

Energy absorbed by the H_2O molecule is almost instantaneously converted to translational energy. Energy absorbed by the CO_2 molecule is trapped in vibrational levels for a longer period of time (approximately 1 ms) (Ref. 12). The CO_2 molecule absorbs very little of the incoming energy, reaching a maximum of 0.2%/m in a density range of less than 1 kg/m^3. Higher densities show negligible absorption. For these reasons, absorption by the CO_2 molecule was omitted from this analysis.

Equation (15) shows that absorption is dependent on the partial pressure of H_2O. To increase H_2O concentrations, the CO_2-laser-based SHX concept assumes injection of H_2 into the engine flowpath at a 50% stoichiometric rate. The injected fuel is assumed to spread uniformly throughout the axial length of the engine. Analyses using the CEA program suggest the reaction of H_2 and air at this O/F ratio will predominately produce H_2O. Even at 4000°R, the equilibrium hydrogen byproducts other than H_2O ($H+$, OH^-, H_3O^+, etc.) comprise less than 1% of the mole fraction of the products. With mixing losses included, it is conservatively assumed that 85% of the injected H_2 is converted to H_2O. The absorption of the incident laser beams is then calculated using the local H_2O partial pressure.

The injection of H_2 causes several changes in the engine flowpath that are not experienced by the other beam heating modes. First, injected H_2 adds mass to the flowpath. However, for a stoichiometric mixture of H_2 with inlet air, the change in mass is less than 3% of the air mass flow rate. This small change is typically ignored for high-level engine analyses and is, therefore, neglected here. Second, the combustion process releases heat into the airstream. The heat released by combustion goes partially to heating the injected hydrogen, which is typically injected at temperatures much colder than that of the working air. To model this effect, a lower combustion efficiency of 60% was used to account for the reduced combustion energy available for heating the working air. Finally, the combustion reaction changes the composition of the working air. If all of the available oxygen is combusted and no radicals are present, the specific R can change nearly 8.5%. This order of error is comparable to the other error sources and is, therefore, neglected.

Electron Beam

The third approach considered for directly heating the SHX airflow is the electron beam. This system projects high-energy electrons into the working air. Energy is imparted through molecular collisions with the electrons. Collision with a much heavier air molecule (N_2 or O_2) tends to deflect an electron from its original trajectory. Therefore, a magnetic field must be generated in a direction perpendicular to the airflow and parallel to the e-beam direction. The field assists the beam in penetrating the working air. In this system, the fusion reaction provides the necessary source of free electrons. The weights of the e-beam generators and peripheral equipment are fully accounted for in the fusion engine mass relations [Eqs. (1–4)].

Energy transfer from the e-beam to the air happens much quicker than the radiative processes in the other two laser-based concepts. Bussard[2] states that the e-beam energy provided in his predictions will be completely absorbed within 0.5 m. Macheret et al.[13] described a system where e-beams are fired from both sides of a duct. The combined effect of both beams generates a relatively uniform heating profile across the majority of the duct. The quasi-one-dimensional SHX model already assumes a uniform heating profile. Several beam emitters would be placed along the length of the combustor in an operational system.

E-beam heating excites the vibrational modes of the N_2 and O_2 molecules in the air.[14] Initially, up to 80% of the absorbed energy is contained in N_2 vibrational modes. These vibrational modes relax primarily through collisions with free oxygen radicals and water

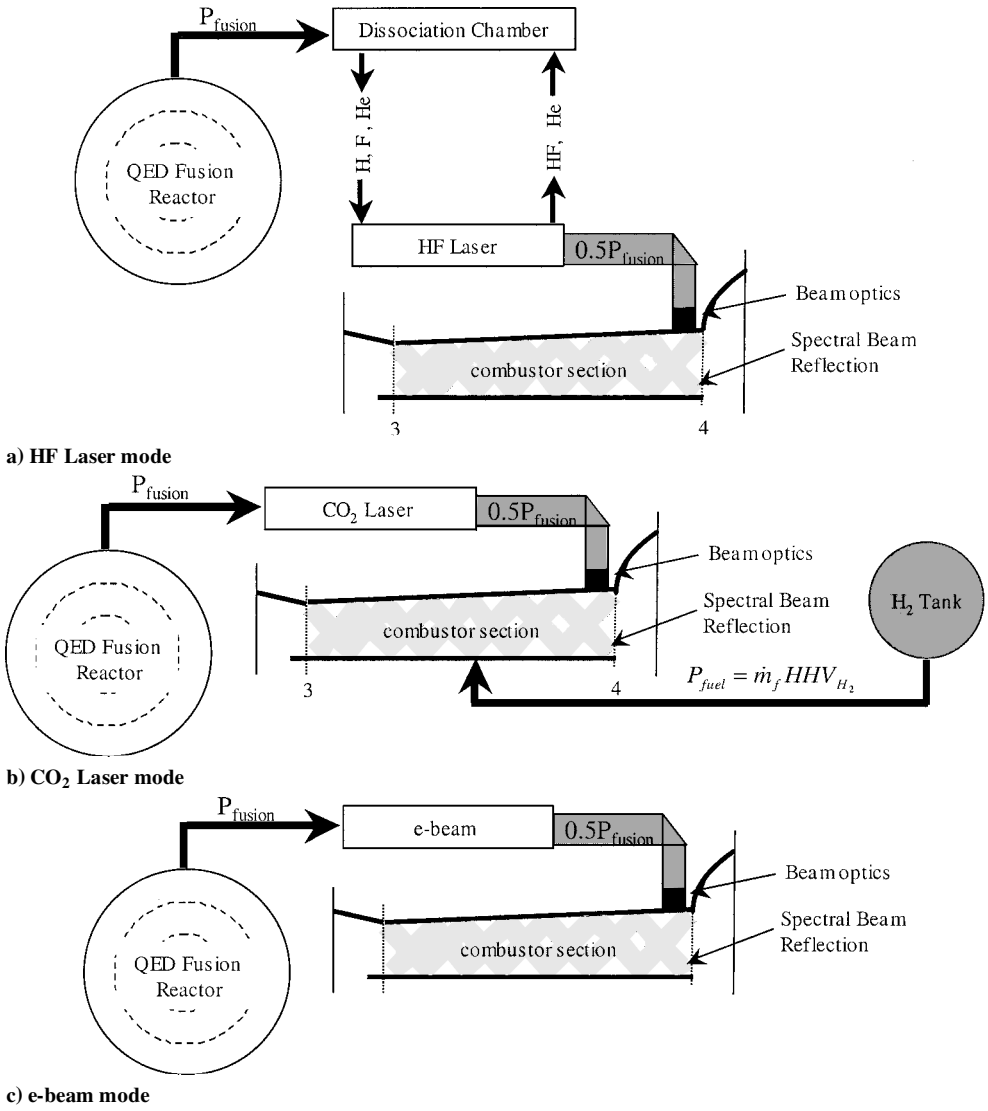

Fig. 7 Power flow diagrams for candidate SHX beam emitter systems.

molecules. Calculating this relaxation time and multiplying by the velocity of the flow yields a minimum distance for the element width in the SHX model.[4] In this manner, an assumption that the input energy is fully relaxed and that vibrational nonequilibrium can be neglected is justified. Furthermore, due to the difficulty in penetrating air with a relativistic e-beam, it is assumed that the beam energy is fully absorbed by the working air.

Concept Summary

Figure 7 illustrates the power flow through the three candidate beam emitters for the SHX engine. In all cases, the fusion reactor produces the necessary power P_{fusion}. The conversion between the electrical energy generated by the reactor to beam energy is assumed to be 50% (Ref. 4). At this point, the SHX operation deviates based on the type of beam emitter.

In the HF laser option (Fig. 7a) the power from the reactor is used to disassociate the HF reactants, which cycle between the laser and a disassociation chamber. The disassociated reactants flow into the lasing cavity. The laser beam is then directed into the engine flowpath. Beam energy absorption is based on the polynomial curve fits shown in Fig. 6.

In the CO_2 laser mode (Fig. 7b) the fusion power is used to drive the electrical discharge across the lasing cavity. Again the conversion efficiency is assumed to be 50%. The CO_2 energy absorption is based on Eq. (15). The fuel power, the product of the mass flow rate and the heating value (HHV_{H2}) of hydrogen, is shown originating from the H_2 tank. The amount of power that actually makes it into the flowpath is the product of the fuel power, the mixing efficiency, and the combustion efficiency. In this study, the beam power for the CO_2 laser was reduced by the fuel power to compare it with the other beam emitter options at the same total power.

Electrical power from the reactor for the e-beam emitter option (Fig. 7c) is converted into a coherent beam with a 50% efficiency. The beam is then directed transversely into the flow. A 100% energy absorption rate is assumed.

Results

Simulation Cases

Most scramjet engines are designed to operate in a Mach number regime of 4.0–12.0 with higher specific impulses at the lower Mach numbers. Trajectories that maximize air mass capture are desirable. By the use of an airbreathing trajectory defined by Billig,[15] SHX and scramjet performance were simulated for a Mach number of 5.0 and an altitude of 65,750 ft.

The power-to-mass relationship for the fusion engine scales favorably with size. Therefore, the maximum benefit of employing a nuclear reactor is only realized when the vehicle is large enough to warrant using such a power system. On the other hand, the ultimate goal of this project is to develop an airbreathing vehicle that can emulate airplane-like operation. The baseline SHX vehicle geometry (see Fig. 1) was designed to be similar in size to the Space Shuttle Orbiter. The airflow passed through a bow shock generated by a wedge-shaped forebody with a 25-deg half-angle. The flow

Table 1 SHX simulation cases

Case	Area profile	Total power, MW	Mode of heating
1	(Bilinear) 1	4000	(HF) 1
2	1	4000	(CO_2) 2
3	1	4000	(e-beam) 3
4	(Parabolic) 2	4000	1
5	2	4000	2
6	2	4000	3
7	(Constant slope) 3	4000	1
8	3	4000	2
9	3	4000	3
10	1	3000	3
11	1	3500	3
12	1	4500	3
13	1	5000	3

was then turned back 25 deg through an inlet shock so that it was parallel to the engine duct. Consistent with the station nomenclature shown in Fig. 1, the combustor length was $l_c = 40.0$ ft. The combustor inlet height and width were 3 and 12 ft, respectively. To alleviate thermal choking, the combustor duct expanded with an area ratio of $A_4/A_3 = 3$. The combustor flow exits to an isentropic expansion surface with a length of $l_e = 50$ ft. The expansion area ratio of $A_{10}/A_4 = 4$ was selected to maintain the exit pressure above the ambient pressure.

Several parameters must be optimized to maximize SHX performance. First, the cross-sectional area profile has a strong effect on the flow properties. Although the inlet and exit areas were kept constant, the effects of the internal change of the area were investigated. The second variable studied was the heating mode (HF laser, CO_2 laser, or the e-beam). Finally, the effect of total heat input on the engine performance was evaluated. Table 1 summarizes the various simulation cases. Both frozen and equilibrium cases were analyzed.

Specific Thrust and Impulse

Figure 8 illustrates the specific thrusts calculated for simulation cases 1–9. Note that the equilibrium chemistry specific thrusts trail those for frozen flow in all cases. As mentioned earlier, the equilibrium calculation accounts for energy that resides in vibrational excitation of the molecules. This energy does not contribute to thrust, and, therefore, the specific thrust is lower. Comparing bilinear area profile (cases 1–3) and the parabolic profile (cases 4–6), it is clear that the parabolic profile provides a more efficient expansion. The constant slope duct (cases 7–9) clearly underperforms the other cases due to fast expansion producing low densities. The lower densities yield lower absorption coefficients and, thus, the working air absorbs less of the incident beam. The more rapid area change in the engine section for the constant slope duct provides less opportunity for isentropic expansion and, therefore, less thrust.

HF-laser heating (cases 1, 4, 7) outperforms the CO_2 laser (cases 2, 5, 8) in all cases except for the bilinear duct. One possible explanation is that the linear expansion profile does not efficiently expand the added energy provided by the HF laser (as compared to the CO_2 laser). Also, the CO_2 laser has a less steep initial heating profile (see Ref. 3). Thus, at the combustor exit (station 4), the CO_2 laser heated flow has not decelerated to the level of the HF laser flow. In cases 4 and 5, the parabolic profile is able to better expand the heated engine flow. In case 7, the constant slope profile alleviates the deceleration effects of the HF heating profile by virtue of the larger cross-sectional area at station 4. The e-beam mode (cases 3, 6, and 9) significantly outperforms the other modes by virtue of its constant heating profile and the assumption of 100% energy absorption.

The reference line shown in Fig. 8 is the specific thrust for an idealized scramjet engine calculated by the HAP program.[1] Input parameters similar to those for the SHX simulations were used, as well as other reference values given on pages 431 and 432 of Ref. 1. To provide a consistent basis for performance comparisons, the scramjet several reference values were modified as follows. First, the ratio of specific heats was set to 1.4 to simulate frozen flow. Second, the fuel heating value ratio was reduced to give an energy input rate (5000 MW) equivalent to the highest rate in the SHX

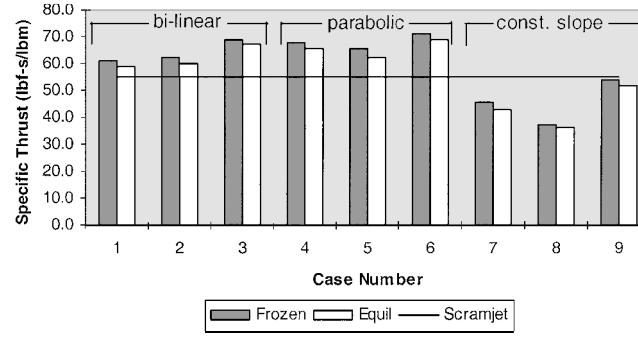

Fig. 8 Effects of area profile and beam emitter on specific thrust for simulation cases 1–9 defined in Table 1.

analysis. Third, inviscid flow was assumed consistent with the SHX model. Under these conditions, a specific thrust of 55.3 lbf · s/lbm and a specific impulse (based on the fuel mass flow rate) of 1898 s were calculated for the scramjet.

E-beam simulation cases 10–13 were designed to investigate the effect of energy input on specific thrust. Along with simulation case 3, these cases employ beam powers varying from 3000 to 5000 MW and use the bilinear area profile (see Table 1). The upper limit of 5000 MW was the maximum energy input allowed without creating a thermal choke in the engine. Results are shown in Fig. 9. The specific thrust linearly increases with energy input. These results suggest that the maximum amount of energy should be input that does not cause choking. Additional energy can be input if the combustor area ratio is raised. However, the combustor area ratio is also limited by geometric constraints.

Figures 8 and 9 reveal several heating mode/area profile combinations (cases 3–6 and 12–13) that perform well above the scramjet. Cases 1 and 2 perform at approximately the same level as the scramjet.

Figure 10 shows the calculated specific impulses for the CO_2 laser mode. This parameter can be determined because H_2 fuel is injected in the airflow. The highest performance is found for case 5, which uses the parabolic area profile. The lowest performance is found for case 8, which uses the constant slope area profile. The variance in performance can be explained by the same reasons as those given for the variance in specific thrusts. All of the cases significantly outperform the specific impulse for the scramjet. This comparison can be misleading, however, because the SHX concepts require mass for the fusion system and beam emitters that is not required by the scramjet and is not included in the calculation of specific impulse.

Thrust-to-Weight Ratio

A discussion of the thrust-to-engine-weight (T/W) results for the SHX concept must be predicated by a detailed analysis of the component masses. The engine weight scales with the design power level as presented in Eqs. (1–4). Recall that 50% conversion efficiency was assumed between the reactor and the beam emitter subsystem. Therefore, the design power level is twice the incident beam power, as listed in Table 1.

The breakdown of the individual engine component weights is shown in Fig. 11. It is evident that the required HF chemical masses dominate the engine mass for this mode. Likewise, the H_2 mass is the dominant portion of the CO_2 laser engine mass. Also note that the beam emitter mass dominates the total engine hardware mass. This suggests that efforts to reduce the engine mass should be concentrated on optimizing the beam emitter subsystem. Despite having the same design power levels, the HF laser mode cases (1, 4, and 7) have substantially different total masses than the e-beam mode cases (3, 6, and 9). The difference is in the required mass of HF products for this laser mode.

The reactor design power levels for the CO_2 laser mode (cases 2, 5, and 8) are substantially lower than for the other cases. This mode derives part of its power from H_2 injection and combustion. Therefore, the beam power and reactor design power were reduced by the power derived from H_2 combustion to maintain a constant total

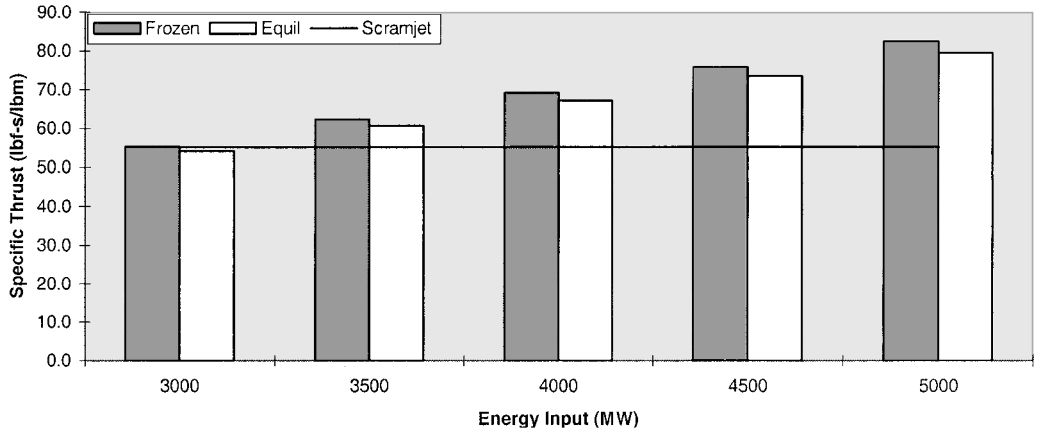

Fig. 9 Specific thrusts for e-beam heating (cases 3 and 10–13) and a bilinear heating profile.

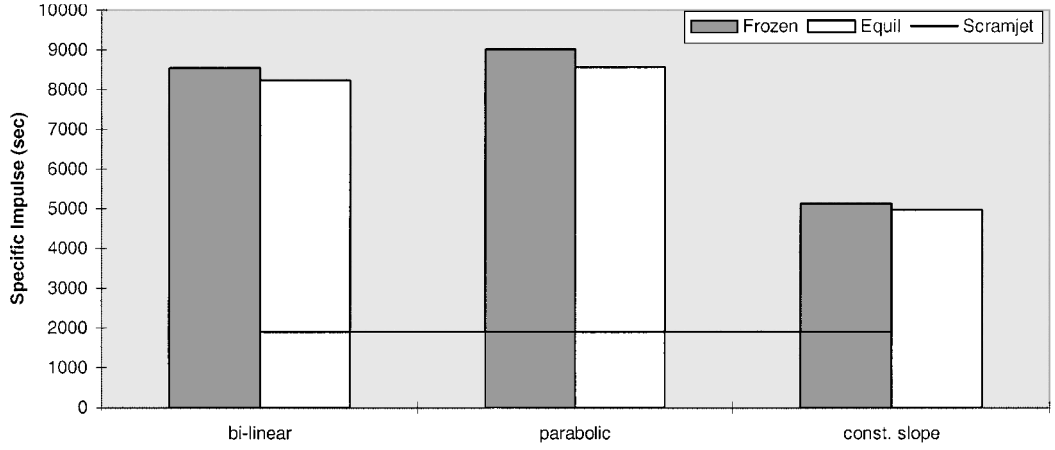

Fig. 10 Specific impulses for CO_2 laser heating cases.

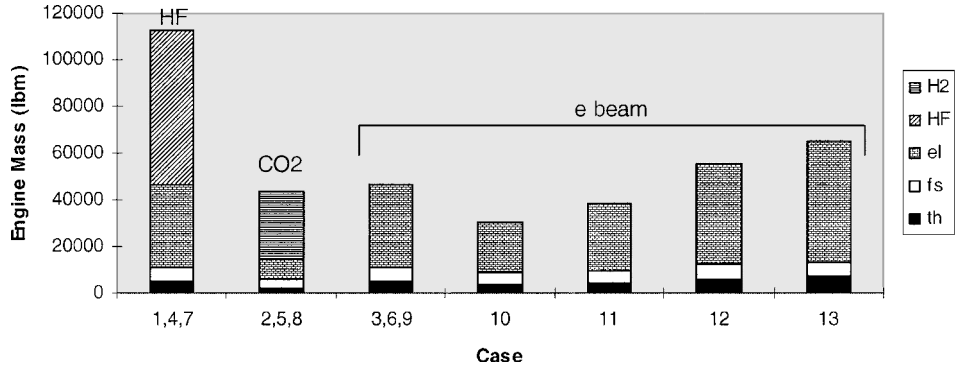

Fig. 11 Engine component masses for simulation cases defined in Table 1.

power. The total mass, including the H_2 propellant, is shown in Fig. 11. The H_2 propellant mass flow rate was calculated using the 50% stoichiometric value and the engine air mass flow rate. Olds et al.[16] suggest state an airbreathing vehicle operates 4–6 min in scramjet mode (from Mach 5 to 12). Using 6 min for the flight time and the H_2 mass flow rate yields a total propellant mass of 29,173 lb. Including propellant mass, this brings the CO_2 laser mode engine weight up to the level of the e-beam mode.

Figure 12 shows the thrust-to-engine-weight ratios calculated for simulation cases 1–9. As noted earlier, for a given beam emitter mode the performance is highest for the parabolic expansion area profile, and the constant slope profile shows the worst performance. Figure 12 also illustrates major variances between the different beam emitter modes. The HF laser cases exhibit the lowest T/W ratios because the added chemical mass more than doubles the total weight of the engine. The CO_2 laser yields the highest T/W ratios due to the lower engine mass for this mode. However, when H_2 propellant weight is added to the engine weight, the resulting T/W ratios slightly lag those of the e-beam modes. This comparison is somewhat misleading because the CO_2 mode will eject propellant in the exhaust. The propellant loss will allow a higher structural mass to be lifted by the CO_2 mode engine.

Comparison of the e-beam cases (3 and 10–13) shows a definite downward trend in the thrust-to-engine-weight ratio with increasing energy input. This is opposite the trend for specific thrust. This result suggests that in designing an e-beam driven SHX vehicle the need for a high T/W must be balanced against the need for a high specific thrust.

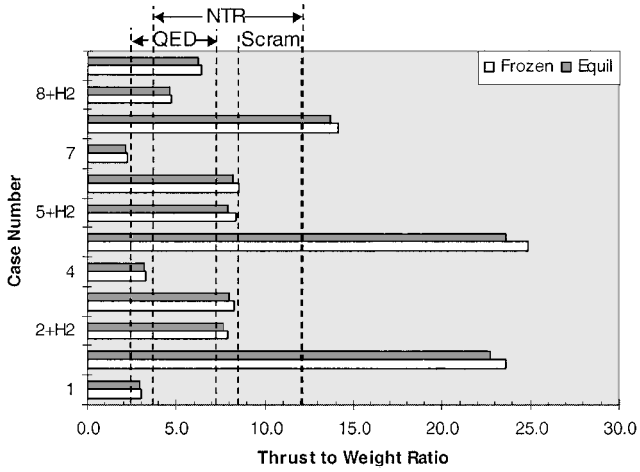

Fig. 12 Thrust to engine weight ratios for SHX simulation cases 1–9 and other propulsion systems.

The T/W values for other existing and proposed propulsion systems are also shown in Fig. 12. Bussard,[2] whose QED rocket engine system serves as the model for the fusion engine of this study, reports thrust to engine weight ratios in the range of 2–6. Borowski et al.[17] outlined a nuclear thermal rocket for a Mars mission with a thrust-to-engine-weight range of 3–10. Sutton[18] gives typical thrust-to-weight ratios of 75 for rockets and 7 for a ramjet. Finally, Kreiger[19] suggests thrust-to-weight ranges of 7–10 for scramjets and 50–100 for rockets. Given these data, the e-beam thrust-to-weight ratios fall within the realm of typical airbreathing engines. Also, the ratios compare favorably to those quoted for the QED rocket engine, suggesting that ducted heating of incoming air could offer a performance improvement over use of onboard propellant.

By the use of the thrust-to-engine-weight ratio without fuel, the CO_2 laser-mode engine significantly outperforms all of the preceding engine concepts except a chemical rocket. Thus, a CO_2 laser-based vehicle could potentially fly a more rocketlike trajectory, cutting down on the thermal protection system requirements. The CO_2 laser performance also suggests that SHX may be more attractive as a secondary propulsion mode, adding energy to combustion gases during airbreathing operation.

The SHX performance simulations are predicated on several assumptions, including frictionless flow, isentropic flow throughout the expansion section, and an inlet operating at design conditions. Heiser and Pratt[1] suggest that including frictional flow and off-nominal expansion have only a secondary effect on airbreathing engine performance. However, the predicted advantages for idealized SHX performance are mitigated somewhat by the conservative assumption of 50% conversion efficiency between the fusion plant and the beam emitter. This drives the fusion plant to be sized for twice the power actually directed into the engine flowpath. Higher conversion efficiencies will almost certainly have to be achieved in practice to avoid rejecting thousands of megawatts of waste energy. Higher conversion efficiencies would also reduce fusion engine weights and, thus, increase thrust-to-weight ratios. Thus, there is good reason to believe that a higher-fidelity model would predict improved SHX performance.

Mission Analysis

The earlier discussion presented design point (Mach 5 and 65,750-ft altitude) performance for the SHX engine concept and compared it to an idealized scramjet. A reasonable attempt was made to quantify engine weights for each of the three beam emitter modes. Mass fraction delivered to orbit is the best measure of the performance of a transatmospheric propulsion system. However, determination of mass fraction requires knowledge of all of the forces acting on the vehicle over a trajectory defined from launch to orbit. The flight trajectory is then optimized to yield the best performance through tradeoffs between the thrust and drag and gravity losses. Weight breakdowns for the various vehicle components are also needed for mission analysis results to be meaningful. This level of detail is beyond the scope of this study. However, generating a comprehensive SHX propulsion deck at various Mach–altitude conditions would provide needed data for follow-on mission analyses.

Conclusions

The various rocket and turbine-based airbreathing propulsion concepts currently under consideration for advanced launch vehicles do not provide the significant performance increases required to meet the aggressive cost goals set by NASA. To meet this need, a novel, advanced airbreathing propulsion system, the SHX engine, is proposed. The SHX uses coherent beam emitters to couple energy generated by a fusion reactor to ingested air. A quasi-one-dimensional model was developed to calculate gasdynamic properties through the engine flowpath. Models were developed for the candidate HF laser, CO_2 laser, and e-beam emitters. A previous study of a fusion rocket was used to derive mass–power relationships for the engine components.

Design point performance for the SHX engine was calculated in terms of specific thrust, specific impulse, and trust-to-engine-weight ratio. Predicted SHX performance was comparable to or slightly better than that of a scramjet engine. Several challenges were identified to maturing the SHX concept to the point of deployment. The issues for the CO_2 and e-beam modes do not appear to be insurmountable. Because of its significant mass requirement, the HF laser mode currently appears to be the least attractive alternative.

The SHX modes would most likely be used in combination with a traditional rocket mode to increase mission-averaged specific impulse. The CO_2 laser mode performance suggests that SHX may be more attractive as a secondary propulsion mode, adding energy to combustion gases during airbreathing operation. However, a detailed mission analysis was not performed in this study.

The results of this study indicate that the SHX concept holds promise for much higher performance gains and is worthy of further study. Note, however, that all of these results are predicated on the successful development of a practical fusion power generator.

Acknowledgments

This study was funded in part through a NASA Phase I Small Business Innovative Research contract awarded to International Space Systems, Inc.

References

[1]Heiser, W. H., and Pratt, D. T., *Hypersonic Airbreathing Propulsion*, AIAA, Washington, DC, 1994, pp. 150, 151.

[2]Bussard, R. W., "The QED Engine System, Direct Electric Fusion Powered Rocket Propulsion Systems," *10th Symposium on Space Nuclear Power and Propulsion*, American Institute of Physics, New York, 1993, pp. 1601–1611.

[3]Gross, R. A., *Fusion Energy*, Wiley, New York, 1984, pp. 16–43.

[4]Adams, R. B., "Preliminary Analysis of a Fusion–Electric Transatmospheric Airbreathing Vehicle," M.S. Thesis, Dept. of Mechanical and Aerospace Engineering, Univ. of Alabama in Huntsville, Huntsville, AL, April 2000.

[5]Adams, R. B., and Landrum, D. B., "Laser–Air Interactions in an Internal Supersonic Flowpath," *Journal of Propulsion and Power*, Vol. 18, No. 4, 2002, pp. 961–963.

[6]Brown, G. L., Ratta, A. P., Anderson, R. W., Martinelli, L., Lempert, W. R., and Miles, R. B., "Fluid Mechanics in a Radiatively Driven Hypersonic Wind Tunnel: Prediction and Preliminary Experiment," AIAA Paper 96-2199, June 1996.

[7]Miles, R. B., Brown, G. L., Lempert, W. R., Yetter, R., Williams, G. J., Jr., Bogdonoff, S. M., Natelson, D., and Guest, G. R., "Radiatively Driven Hypersonic Wind Tunnel," *AIAA Journal*, Vol. 33, No. 8, 1995, pp. 1463–1470.

[8]Rothman, L. S., "HAWKS: HITRAN Atmospheric Workstation 1996 Edition," Ontar Corp., North Andover, MA, 1996.

[9]Macheret, S., Meinrenken, C., Williams, G., Lempert, W., Gillespie, W., Lempert, W., and Miles, R., "Radiative Energy Addition to High Pressure Supersonic Air," AIAA Paper 96-1984, July 1996.

[10]McBride, B. J., and Gordon, S., "Computer Program for Calculation of Complex Chemical Equilibrium Compositions and Applications," NASA RP-1311, 1996.

[11]Gastaud, H., Brunet, H., Voignier, F., and Bousselet, P., "Experimental Study of a Continuous Wave HF Chain Reaction Laser," *Gas-Flow and Chemical Lasers*, McGraw–Hill, New York, 1979, pp. 217–224.

[12]Duley, W. W., *CO_2 Lasers, Effects and Applications*, Academic Press, New York, 1976, pp. 15–21.

[13]Macheret, S. O., Shneider, M. N., Miles, R. B., Lipinski, R. L., and Nelson, G. L., "Magnetohydrodynamics Acceleration of Supersonic Air Flows Using Electron Beam-Enhanced Conductivity," AIAA Paper 98-2922, June 1998.

[14]Macheret, S. O., Ionikh, Y. Z., Martinelli, L., Barker, P. F., and Miles, R. B., "External Control of Plasmas for High-Speed Aerodynamics," AIAA Paper 99-4853, Nov. 1999.

[15]Billig, F. S., "Propulsion Systems from Takeoff to High-Speed Flight," *High-Speed Flight Propulsion Systems*, AIAA, Washington, DC, 1991, pp. 21–100.

[16]Olds, J., Bradford, J., Charania, A., Ledsinger, L., McCormick, D., and Sorensen, K., "Hyperion: An Single Stage to Orbit Vision Vehicle Concept Utilizing Rocket-Based Combined Cycle Propulsion," AIAA Paper 99-4944, Nov. 1999.

[17]Borowski, S. K., Dudzinski, L. A., and McGuire, M. L., "Vehicle and Mission Design Options for the Human Exploration of Mars/Phobos Using Bimodal Nuclear Thermal Rocket and LO_x Augmented Nuclear Thermal Rocket Propulsion," AIAA Paper 98-3883, July 1998.

[18]Sutton, G. P., *Rocket Propulsion Elements*, Wiley, New York, 1992, p. 3.

[19]Krieger, R. J., "A Summary of Features and Design Issues for Single Stage to Orbit Vehicles," AIAA Paper 90-1932, July 1990.